UC Merced

Proceedings of the Annual Meeting of the Cognitive Science Society

Title

How Different Frames of Reference Interact: A Neural Network Model

Permalink

https://escholarship.org/uc/item/6xh4b8js

Journal

Proceedings of the Annual Meeting of the Cognitive Science Society, 38(0)

Authors

Nan, Weizhi
Sun, Yanlong
Liu, Xun
et al.

Publication Date

2016

Peer reviewed

How Different Frames of Reference Interact: A Neural Network Model

Weizhi Nan (nanwz@psych.ac.cn)[a],
Yanlong Sun (ysun@tamhsc.edu)[b],
Xun Liu (liux@psych.ac.cn)[a],
Hongbin Wang (hwang@tamhsc.edu)[b]
[a] Key Laboratory of Behavioral Science, Institute of Psychology,
Chinese Academy of Sciences, 16 Lincui Road, Chaoyang District, Beijing 100101, China
[b] Center for Biomedical Informatics, Texas A&M University Health Science Center,
2121 West Holcombe Blvd, Houston, TX 77030, USA

Abstract

It has been argued that people use multiple frames of reference (FORs) for representing and updating spatial relationships between objects in a complex environment. When there are conflicts among representations of multiple FORs, they compete to determine behavior. "Frame of Reference-based Map of Salience" theory (FORMS) suggests that FORs with high salience may be processed in priority. Here, we report a computational neural network model for a two-cannon task, which naturally involves multiple FORs with different levels of salience: intrinsic frame of reference (IFOR) and egocentric frame of reference (EFOR). The goal is to investigate the computational neural mechanisms underlying human spatial performance. Our simulation results fit earlier behavioral results well. The model suggests although multiple FORs may be initially represented independently, they interfere with each other by the inhibitory competition of neurons in the later process (in hidden layer) for conflict resolution. Moreover, salience may modulate the competition by prioritizing FORs with high salience levels. These results represent a connectionist support for the FORMS theory.

Keywords: frame of reference; inhibitory competition; salience; neural network model

Introduction

People adopt multiple frames of reference (FORs) to represent the spatial relationship of objects in a complex environment (Klatzky, 1998; Mou & McNamara, 2002; Piaget & Inhelder, 1956; Sun & Wang, 2014; Tamborello, Sun, & Wang, 2012; Wang, Johnson, & Zhang, 2001; Zacks & Michelon, 2005). Based on the relationship with the observer, FORs can be classified into three types, egocentric FOR (EFOR), intrinsic FOR (IFOR) and allocentric FOR (AFOR) (Klatzky, 1998; Mou & McNamara, 2002; Tamborello et al., 2012; Wang & Spelke, 2002). An EFOR-based representation is anchored to the observer, which needs to be updated following the movement of the observer's eye, head, body coordinates (Wang et al., 2001). In an IFOR-based representation, an object or an object group in the viewing environment but exogenous to the observer is used as the reference point. For example, a table is used as an IFOR anchor in the description "the cup is on the table". IFORs remain stable with the observer's movement but have to be updated when the reference object moves. In an AFOR-based representation, the entire environment, such as a room or a city, is taken as the

reference point. For a comprehensive review, see (Mou, Fan, McNamara, & Owen, 2008; Mou & McNamara, 2002; Sun & Wang, 2010, 2014; Tamborello et al., 2012; Yamamoto & Philbeck, 2013).

Particularly of our interests is how multiple FOR representations develop and interact with each other. Mathematically, all FORs are equivalent. Depending on specific situations, however, some FORs are more useful or convenient. In comparison, EFOR is probably more automatic and almost effortless, AFOR is quite stable but computationally demanding, and IFOR is a balance between flexibility and stability. "Frame of Reference-based Map of Salience" theory (FORMS) states the human brain represents spatial information simultaneously using multiple FORs, each being a spatial map of salience (i.e. only salient objects or locations are represented on each map), and that human performance is determined by the interaction of all relevant FOR-based representations (Sun & Wang, 2010, 2014; Tamborello et al., 2012; Wang et al., 2001; Wang, Sun, Johnson, & Yuan, 2005; Yamamoto & Philbeck, 2013).

To understand the interaction among multiple FORs and the effect of salience, Tamborello et al. (2012) designed a two-cannon task (a modified and simplified version is shown in Figure 1), in which two cannons (a red and a blue) were surrounded by 8 pellets in red or blue color. The salience of the cannons was determined by the pellet color ratio such that the cannon with more same-color pellets was more salient. In the task, when one of the pellets was randomly chosen as the target pellet (flashing), the cannon in the same color became the target cannon. Participants were asked to rotate the target cannon to the location of the flashing target pellet in the shortest way by pressing either the left-arrow or the right-arrow button on the keyboard. An analysis (Figure 3A and 3B) showed that reaction time (RT) became longer when there was a conflict among different FOR-based representations. RT in cannon angle 180° condition was longer than RT in cannon angle 0° condition (Cannon Angle Effect). In the cannon angle 180° condition, RT for trials where the target pellet appeared in the minority color group was longer than RT for those in the majority color group (Salience Effect). RT in target cannon point-down condition was longer than RT in target cannon point-up condition (Target Cannon Orientation Effect). And the target cannon orientation effect was larger in cannon angle 180° condition than that in cannon angle 0° condition,

Figure 1. A schematic illustration of the two-cannon task. Middle: trial procedure. At the beginning of each trial, a fixation cross was presented at the center of the screen for 500 ms, and subjects were asked to fixate on it, then two cannons (one red and one blue) and eight pellets (in either red or blue) were presented together on the computer screen. After a one-second pause, a randomly selected pellet would flash as the target pellet. The participants' task was to use the arrow keys to rotate the cannon in the same color of the target pellet toward the target pellet as quickly as possible. Auditory feedback was played for either the correct (a shot sound) or incorrect (an alarm sound) response; top left: cannon congruent (0°) and cannon incongruent (180°); top right: pellet color ratio (blue : red = 6:2, 4:4, and 2:6); bottom left: likely target pellet (target occurs in the majority color pellets) and less likely target pellet (target occurs in the minority color pellets); bottom right: target cannon orientation up (12 o'clock is 0°, clockwise rotation, set 315°, 0°, and 45° as the target cannon up condition) and down (set 135°, 180°, and 225° as the target cannon down condition).
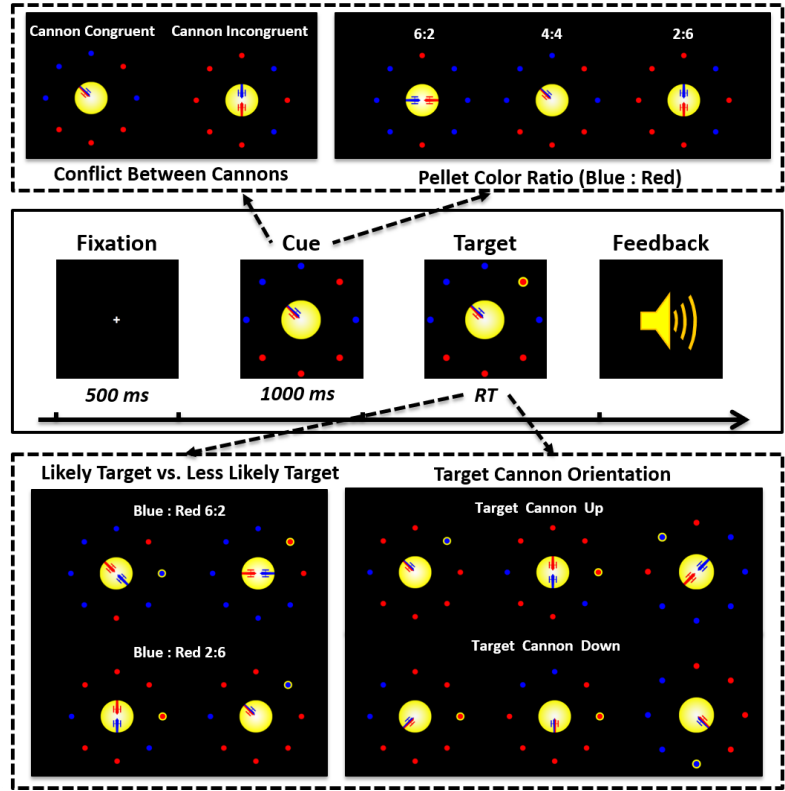

Table 1. The training data for the model. Each row represents a group of trials that covers different FORs with different orientations and salience, different target pellet color. The first three columns ("FOR number", "Cannon Angle" and "Pellet Ratio B:R") represent different conditions; Column "Weights" represents relative frequency; Column "Types" represents how many trial types are contained in each group; the last ten columns represent specific input information, with salience level ranging from 0.2 to 0.8, and cannon orientation or target location as up-right (UR), up (U), down-left (DL), or down-right (DR); the last column is the response (right or left key).

FOR Number	Cannon Angle	Pellet Raito B:R	Weights	Types	Blue Cannon Orientation	Blue Cannon Salience	Red Cannon Orientation	Red Cannon Salience	EFOR Orientation	EFOR Salience	Blue Target Pellet	Target Pellet Location	Red Target Pellet	Output
3FORs	0°	2:6	1	36	UR	0.2	UR	0.8	U	0.5		DR	1	Right
3FORs	0°	2:6	1	36	UR	0.2	UR	0.8	U	0.5	1	DR		Right
3FORs	0°	4:4	1	36	UR	0.5	UR	0.5	U	0.5		DR	1	Right
3FORs	0°	4:4	1	36	UR	0.5	UR	0.5	U	0.5	1	DR		Right
3FORs	0°	6:2	1	36	UR	0.8	UR	0.2	U	0.5		DR	1	Right
3FORs	0°	6:2	1	36	UR	0.8	UR	0.2	U	0.5	1	DR		Right
3FORs	180°	2:6	3	36	UR	0.2	DL	0.8	U	0.5		DR	1	Left
3FORs	180°	2:6	1	36	UR	0.2	DL	0.8	U	0.5	1	DR		Right
3FORs	180°	4:4	1	36	UR	0.5	DL	0.5	U	0.5		DR	1	Left
3FORs	180°	4:4	1	36	UR	0.5	DL	0.5	U	0.5	1	DR		Right
3FORs	180°	6:2	1	36	UR	0.8	DL	0.2	U	0.5		DR	1	Left
3FORs	180°	6:2	3	36	UR	0.8	DL	0.2	U	0.5	1	DR		Right
EFOR			50	6					U			DR		Right

which means there was an interaction between cannon angle effect and target cannon orientation effect. These results indicate that people encounter difficulties when they have to process different conflicting FOR representations and that they seem to prioritize processing of each FOR by salience.

How the conflicts occur raises an issue. In particular, how are the conflicts among FORs represented and what is the mechanism of conflict resolution? Previously, we have hinted that spatiotemporal association and predictive learning play a major role in such tasks (Sun & Wang, 2014). In the current study, we evaluate the hypothesis by developing a neural network model of the two-cannon task. The model is implemented in Leabra (local, error-driven and associative, biologically realistic algorithm), a biologically based computational modeling framework (O'Reilly, 1998; O'Reilly, Munakata, Frank, & Hazy, 2012). Among all the features, Leabra incorporates complex network dynamics using bidirectional excitatory connections and fast pooled inhibition, which makes it an ideal candidate for exploring the interference among conflicting cognitive process.
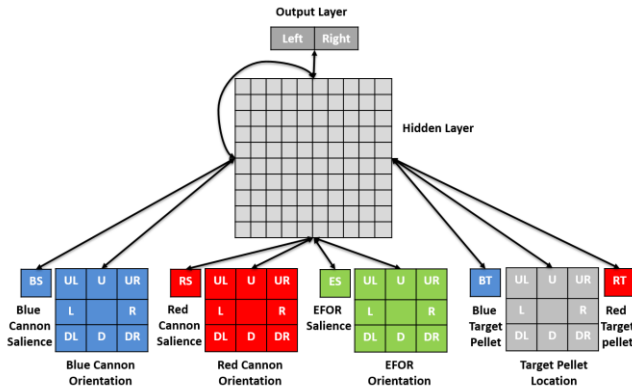
Figure 2. The model of the two-cannon task. Three 3x3 FOR orientation layers (excluding the center neuron, the other eight neurons corresponding to eight orientations: U-up, UR-up-right, R-right, DR-down-right, D-down, DL-down-left, L-left, UL-up-left) with three 1x1 salience layer; one 3x3 target pellet location layer (excluding the center neuron, the other neurons corresponding to eight locations) with two 1x1 target pellet color layer (representing the color of the target pellet); one 10x10 hidden layer; one 2x1 output layer (Left, Right).

The Neural Network Model

Model Architecture and Connectivity

The model (Figure 2) consists of three levels of layers (input, hidden and output). At the input level, there are nine input layers. Each layer encodes one piece of stimulus information independently. Three 3x3 layers are used to encode the orientations of two IFORs and one EFOR (Blue Cannon Orientation, Red Cannon Orientation and EFOR Orientation in Figure 2). Three 1x1 layers aside the three FOR input layers are used to encode their salience (Blue Cannon Salience, Red Cannon Salience, EFOR Salience). One 3x3 layer filled in gray color is used to encode the locations of target pellet (Target Pellet Location). Two 1x1 layers aside the target location input layer are used to encode the color of target pellet (Blue Target Pellet, Red Target Pellet). At the hidden level, one 10x10 layer is used to represent and process all the vision input information. At the output level, one 2x1 layer is used to encode the response.

The connections among the layers are all bi-directional. The hidden layer has a self-recurrent excitatory connection to itself. The weight of forward connection is stronger than the weight of the feedback and self-recurrent excitatory connection with a ratio of 2:1. The k-winner-take-all parameter is used in the hidden layer (the percentage, k= 25%) and the output layer (the number of neurons, k= 1), which controls the activation level of the two layers without using explicit inhibitory neurons. All other parameters used in the model take the default values of Leabra (O'Reilly et al., 2012).

Training and Testing

The training data set consists of 13 groups of trials (Table 1). The first 12 groups are used to train the three FORs-coexisting conditions and the last group is for the single EROR condition. The first 12 groups are generated based on three independent variables: cannon angle (0°, 180°), the pellet color ratio (blue: red = 2:6, 4:4, and 6:2), and target pellet color (Blue, Red). The orientations of each cannon (shown in "Blue Cannon Orientation" column and "Red Cannon Orientation" column, same orientations for cannon angle 0° condition, opposite orientations for cannon angle 180° condition) control the cannon angle (shown in "Cannon Angle" column). The pellet color ratio (shown in "Pellet Ratio B: R" column) will change the salience of each cannon (shown in "Blue Cannon Salience" column and "Red Cannon Salience" column. e.g. if blue: red= 2:6, we set 0.2 for blue salience and 0.8 for red salience). The target pellet color (shown in "Blue Target Pellet" column and "Red Target Pellet" column) controls the target pellet color of each trial and the blue/red target pellet also indicates the correct response should be made by the blue/red cannon. In each of the 12 groups, there are 36 trial types separated by the cannon orientation and target pellet location (shown in "Types" column. 8 cannon orientations and different target pellet location excluding locations same with or opposite to cannon and EFOR orientations). In order to increase the robustness of salience effect, we set the salience groups 3 times more than the other groups (shown in "Weights" column).

EFOR is always automatic activated as the point-up orientation because in behavioral studies participants ("observers") were always facing with the computer screen. When the target cannon points above the horizontal, the target cannon's IFOR matches the participant's EFOR; when it points below the horizontal, IFOR does not match EFOR, causing a conflict between IFOR and EFOR (Target Cannon Orientation Effect). Thus, we set the last group for the EFOR, and specially train the single EFOR with an only point-up orientation group. In EFOR group, there are 6 trial types (1 EFOR orientation and 6 target pellet location excluding locations same with or opposite to EFOR orientation). In order to increase the robustness of the effect, we set the weight of the EFOR group as 50. The total trial number of training data is (1*10+3*2) *36+50*6=876. And the testing data contains only three FORs coexisting groups, and each group only repeats by one time, so the total trial number of testing data is 12*36=432.

We set the maximum cycles of each trial as 200. If the cycle reaches 200, the current training trial would stop and switch to next trial. The stop criterion of the whole training is the average sum square error (SSE) reaching 0 by four times continuously. In the testing phase, when the activation of output layer reaches a set threshold (0.85) a response is said to have been made. The number of cycles is taken as the measure of model RT.

Thirty "simulated subjects", each with randomly initialized weights were trained and tested to get thirty independent simulation results.

Simulation Results

Analysis

The dependent variable is the number of computational cycles of each trial. The independent variables are cannon angle (0°, 180°), target cannon orientation (Up, Down), pellets color ratio (Blue: Red = 2:6, 4:4, 6:2), target pellet color (Red, Blue). One 2 (cannon angle) × 3 (pellet color ratio) × 2 (target pellet color) repeated-measures ANOVA was performed on the cycles to search for the main effects of cannon angle effect and the salience effect (Figure 3C. and Table 2). A 2 (cannon angle × 2 (target cannon orientation) repeated-measures ANOVA was performed on the cycles to search for the main effects of target cannon orientation effect, cannon angle effect, and their interaction (Figure 3D and Table 3). A correlation analysis was performed on the simulation results and the behavioral results (Figure 4). According to the FORMS theory and the earlier behavioral experimental results, we expected our model could learn from the training data, and the simulation results would have a positive correlation with earlier behavioral experimental results. The effects of interest are summarized below.

Cannon Angle Effect and Salience Effect

In Figure 3C and Table 2, there was a significant main effect of cannon angle effect, $F (1, 29) = 719.96$, $p < .001$, $\eta p2 = .96$, indicating that the cycles in the cannon angle 0° condition (23.51 ± 0.07) were fewer than the cycles in the cannon angle 180° condition (26.28 ± 0.11). There was a significant interaction of pellet color ratio and target pellet color, $F (2, 58) = 9.10$, $p < .001$, $\eta p2 = .24$. Post hoc analysis suggested that the pattern as below: the cycles of the red target pellet (24.81 ± 0.12) were marginally fewer than that of the blue target pellet (25.09 ± 0.13) in the blue: red = 2:6 condition, $p = .09$. In contrast, cycles of the red target pellet (25.01 ± 0.13) had a trend to be larger than that of the blue target pellet (24.77 ± 0.11) in the blue: red = 6:2 condition, $p > .05$. The cycles of the two target pellet colors (red target pellet: 24.89 ± 0.11, blue target pellet: 24.82 ± 0.11) showed no difference in the blue: red = 4:4 condition, $p > .05$. This interaction pattern only appeared significantly in the cannon angle 180° condition and not in the cannon angle 0° condition, as revealed by the significant three-way interaction among cannon angle, target pellet color, and pellet color ratio, $F (2,58) = 47.84$, $p < .001$, $\eta p2 = .62$. Post hoc analysis in cannon angle 180° condition suggested that the pattern as below: the cycles of the red target pellet (25.96 ± 0.99) were fewer than that of the blue target pellet (26.82 ± 1.15) in the blue: red = 2:6 condition, $p < .01$. In contrast, cycles of the red target pellet (26.63 ± 1.06) were larger than that of the blue target pellet (25.90 ± 0.88) in the blue: red = 6:2 condition, $p < .01$. The cycles of the two

target pellet colors (red target pellet: 26.20 ± 0.79, blue target pellet: 26.18 ± 0.91) showed no difference in the blue: red = 4:4 condition, $p > .05$. No other significant effects were obtained, $ps > .05$.
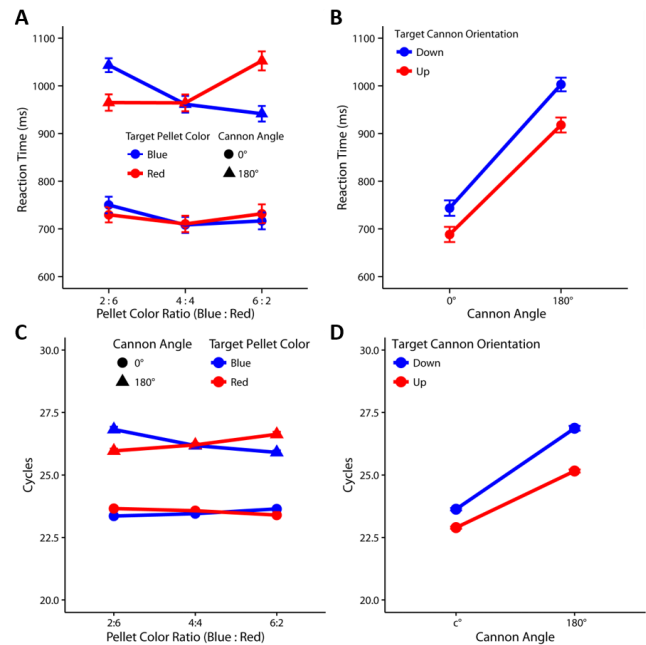

Figure 3 A. RTs for target pellet color, pellet color ratio and cannon angle in behavioral results; B. RTs for target cannon orientation and cannon angle in behavioral results; C. Cycles for target pellet color, pellet color ratio and cannon angle in simulation results; D. Cycles for target cannon orientation and cannon angle in simulation results.

Table 2: Cycles of target pellet color, pellet color ratio, and cannon angle

Cannon angle	Target pellet color	Pellet color ratio blue: red		
		2:6	4:4	6:2
180°	blue	26.82±1.15	26.18±0.91	25.90±0.88
	red	25.96±0.99	26.20±0.79	26.63±1.06
0°	blue	23.36±0.52	23.45±0.52	23.64±0.53
	red	23.66±0.50	23.57±0.60	23.40±0.51

Table 3: Cycles of target cannon orientation and cannon angle

Target cannon orientation	Cannon angle	
	0°	180°
Down	23.63±0.52	26.87±1.03
Up	22.89±0.48	25.16±0.65

Target Cannon Orientation Effect and Cannon Angle Effect

The cycles results (Figure 3D and Table 3) showed significant main effects for target cannon orientation effect

and cannon angle effect [F (1, 29) = 75.82, p < .001, ηp2 = .72; F (1, 29) = 717.79, p < .001, ηp2 = .96]. The interaction of the two factors was also significant, F (1, 29) = 25.03, p < .001, ηp2 = .46. Post hoc analysis suggested that target cannon orientation effect in the cannon angle 180° condition (1.71 ± 0.20) was larger than the effect in the cannon angle 0° condition (0.74 ± 0.13).

Correlation

A correlation analysis between the simulation results and behavioral results was conducted. For cannon angle effect and salience effect, we combined all the 12 conditions (target color × cannon angle × pellet color ratio) together to analyze the relation among these conditions. It is evident results (Figure 4A) that there was a significantly positive correlation, r = 0.53, p < .01, df = 358. For the cannon angle effect and target cannon orientation effect, we combined the 4 conditions (target cannon orientation × cannon angle) together to analyze the relation among these conditions. Results (Figure 4B) showed that there was also a significantly positive correlation, r =.56, p < .01, df = 118.
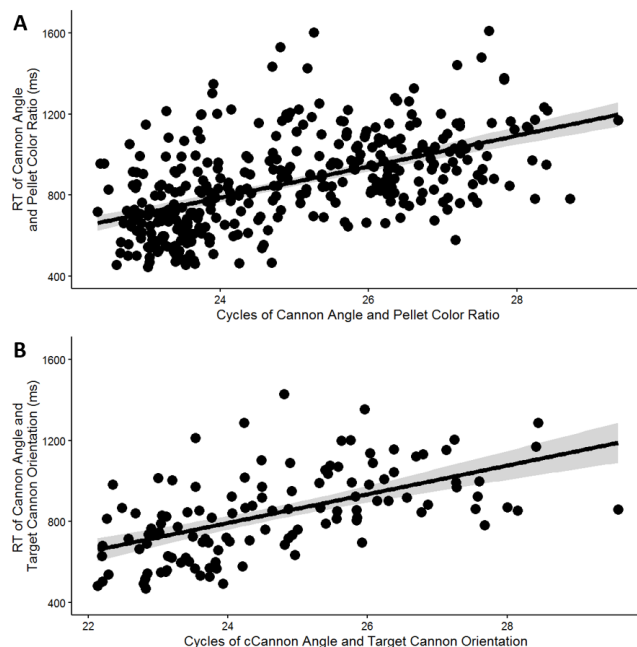

Figure 4 A. Correlation in target color, cannon angle and pellet color ratio; B. Correlation in target cannon orientation and cannon angle.

Discussion

The results from the neural network model of the two-cannon task are consistent with our earlier interpretations of the behavioral results based on the FORMS theory. The model shows stable performance and replicates all major effects with a close match to the behavioral results. Importantly, these results provide a neural basis to our theory where we can characterize the competition between different FOR-based representations by inhibitory competition among groups of neurons and predictive learning.

According to the FORMS theory, multiple representations with respect to different FORs may co-exist in a segmented but competitive fashion. The salience of any particular representation is driven by not only the perception of a static scene (e.g., the ratio between blue and red pellets) but also the prediction of the changing environment (e.g., a red cannon would be more likely to be the target cannon because there are more red pellets). This means that in a complex environment with multiple spatial relationships, representations anchored to different FORs have to be constantly maintained and updated. The simulation results from the neural network model suggest that the process of maintenance and updating can take place distributive within the same group of neurons (hidden layer), and therefore afford the possibility of interference among different FOR-based representations at the neural level.

The model showed the cannon angle effect, target cannon orientation effect and the interaction between them. The cannon angle effect was demonstrated by the fewer cycles in the cannon angle 0° condition (the orientation of the potential IFOR was the same as the orientation of the target IFOR) than in the cannon angle 180° condition (the orientation of the potential IFOR was opposite to the orientation of target IFOR). And the target cannon orientation effect was revealed by the fact that the cycles of the target cannon point-up condition (the orientation of target IFOR was the same as the orientation of EFOR) were fewer than that of the target cannon point-down condition (the orientation of target IFOR was opposite to the orientation of EFOR). These two effects suggest that in the hidden layer, there may be the same group of neurons responsible for computing the output based on the different FORs (blue cannon anchored to blue IFOR, red cannon anchored to red IFOR and observer anchored to EFOR). Therefore, when the orientation of the target IFOR was same as the orientation of the potential IFOR or EFOR, the response became faster. On the contrary, when their orientations were different, inhibitory competition occurred, and neurons took more time to focus on the target IFOR, leading to slower responses. In addition, the interaction between the two effects was revealed by the larger target cannon orientation effect in cannon angle 180° condition than that in cannon angle 0° condition. According to the adding factor theory, when two processes occur in the same phase, they will compete with each other for the cognitive resource, resulting in longer RT (Liu, Banich, Jacobson, & Tanabe, 2004; Liu, Park, Gu, & Fan, 2010; Sternberg, 1969). In this study, it is likely that some shared neurons for FOR information processing in the hidden layer give rise to these effects. The salience effect was demonstrated by fewer cycles in the likely target pellet condition than that in the less likely target pellet condition. We hypothesize that neurons in the hidden layer learned to predict the cannon with the same color of majority pellets as the target cannon.

If the prediction was right, the response would be fast. If the prediction was incorrect, it would take more time to update the target cannon, so the response would be slow. The salience level associated with each FOR might enhance the competition and lead to a prioritization of the corresponding FOR. However, it was the real-time prediction and inhibitory competition that contributed to the extra computational time for resolving potential conflicts (Sun & Wang, 2014).

The above analysis suggests that the interaction among neuron groups in the hidden layer may be responsible for the modeling results. The next step is to perform further data analysis, such as PCA and cluster analysis to evaluate these predictions. Another step is to add the cue data to the testing data set to make the model process the input information in temporal sequences. Then the predictive learning and the target decision making could be more clearly separated in the model.

Conclusion

Our neural network model replicates the behavioral results well, supporting the claim that representations with multiple FORs co-exist and compete to determine performance. Importantly, it suggests a plausible neural mechanism underlying the FORMS theory. Depending on whether there are conflicts among different FOR representations and whether the actual outcome is consistent with the expectation, competition takes place at different levels and results in the engagement and disengagement of different FOR-based representations. According to the salience effect, the internal spatial representation of the environment is always dynamically constructed and updated toward the anticipated outcomes, rather than just representing static associations of the current spatial configuration. These results support our interpretation of spatiotemporal association and predictive learning.

Acknowledgments

References

Klatzky, R. L. (1998). *Allocentric and egocentric spatial representations: Definitions, distinctions, and interconnections.* Paper presented at the Spatial cognition.

Liu, X., Banich, M. T., Jacobson, B. L., & Tanabe, J. L. (2004). Common and distinct neural substrates of attentional control in an integrated Simon and spatial Stroop task as assessed by event-related fMRI. *Neuroimage, 22*(3), 1097-1106.

Liu, X., Park, Y., Gu, X., & Fan, J. (2010). Dimensional overlap accounts for independence and integration of stimulus-response compatibility effects. *Atten Percept Psychophys, 72*(6), 1710-1720.

Mou, W., Fan, Y., McNamara, T. P., & Owen, C. B. (2008). Intrinsic frames of reference and egocentric viewpoints in scene recognition. *Cognition, 106*(2), 750-769.

Mou, W., & McNamara, T. P. (2002). Intrinsic frames of reference in spatial memory. *J Exp Psychol Learn Mem Cogn, 28*(1), 162-170.

O'Reilly, R. C. (1998). Six principles for biologically based computational models of cortical cognition. *Trends in Cognitive Sciences, 2*(11), 455-462.

O'Reilly, R. C., Munakata, Y., Frank, M., & Hazy, T. (2012). *Computational cognitive neuroscience*: PediaPress.

Piaget, J., & Inhelder, B. (1956). The child's concept of space. *New York: Humanities Pr*.

Sternberg, S. (1969). The discovery of processing stages: Extensions of Donders' method. *Acta Psychologica, 30*, 276-315.

Sun, Y., & Wang, H. (2010). Perception of space by multiple intrinsic frames of reference. *Plos One, 5*(5), e10442.

Sun, Y., & Wang, H. (2014). Insight into others' minds: spatio-temporal representations by intrinsic frame of reference. *Frontiers in Human Neuroscience, 8(58)*, 1-11.

Tamborello, F. P., 2nd, Sun, Y., & Wang, H. (2012). Spatial reasoning with multiple intrinsic frames of reference. *Experimental Psychology, 59*(1), 3-10.

Wang, H., Johnson, T. R., & Zhang, J. (2001). *The mind's views of space.* Paper presented at the Proceedings of the Third International Conference of Cognitive Science.

Wang, H., Sun, Y., Johnson, T. R., & Yuan, Y. (2005). Prioritized spatial updating in the intrinsic frame of reference. *Spatial Cognition and Computation, 5*(1), 89-113.

Wang, R., & Spelke, E. (2002). Human spatial representation: insights from animals. *Trends in Cognitive Sciences, 6*(9), 376.

Yamamoto, N., & Philbeck, J. W. (2013). Intrinsic frames of reference in haptic spatial learning. *Cognition, 129*(2), 447-456.

Zacks, J. M., & Michelon, P. (2005). Transformations of visuospatial images. *Behav Cogn Neurosci Rev, 4*(2), 96-118.